Noise in Magnitude Magnetic Resonance Images

ARTURO CÁRDENAS-BLANCO,[1] CRISTIAN TEJOS,[2,3] PABLO IRARRAZAVAL,[2,3] IAN CAMERON[1,4]

[1]*Ottawa Health Research Institute, Ottawa, ON, Canada*
[2]*Department of Electrical Engineering, Pontificia Universidad Católica de Chile, Santiago, Chile*
[3]*Biomedical Imaging Center, Pontificia Universidad Católica de Chile, Santiago, Chile*
[4]*Department of Physics, Carleton University, Ottawa, ON, Canada*

ABSTRACT: The aims of this article are to review the properties of noise in magnitude MR images to clarify the terminology used when referring to the noise and to discourage the use of the terms R*ician noise* and R*ician noise bias*. The distribution of measured MR pixel intensities in the presence of noise is known to be Rician, and the width of this distribution is directly related to the Gaussian noise on the measured real and imaginary signals. It is the pixel magnitude values that follow the Rician distribution, not the noise. The term R*ician noise* should be used cautiously or, better still, avoided completely since inherent to this terminology is behavior that is not normally associated with noise, such as dependence on signal strength. This terminology is misleading and can lead to conceptual and practical misunderstandings. It is better to relate the image noise to the Gaussian noise on the real and imaginary signals. Concepts Magn Reson Part A 32A: 409–416, 2008.

KEY WORDS: Rician distribution; Rayleigh distribution; Gaussian distribution; noise; magnitude image formation

INTRODUCTION

It has been noted by the authors that the terms *Rician noise* and *Rician noise bias* are appearing more frequently in the MRI literature. Last year alone, at the ISMRM conference held in Berlin, at least 21 abstracts used one of these expressions when referring to the noise in magnitude MR images or the noise induced bias of the pixel intensities that occurs in magnitude MR images for low SNR. Unfortunately, these expressions inherently attribute properties to the noise which differ from those normally associated with noise. This can lead to incorrect data processing if these effects are not dealt with properly. The intention of the authors is not to disapprove of existing works that use these expressions but rather to make the readers aware of the true statistical nature of noise in MR magnitude images so that in the future more appropriate, unambiguous terminology will be used.

Received 18 January 2008; revised 4 June 2008; accepted 7 August 2008

Correspondence to: Ian Cameron; E-mail: icameron@ottawahospital.on.ca

Concepts in Magnetic Resonance Part A, Vol. 32A(6) 409–416 (2008)

Published online in Wiley InterScience (www.interscience.wiley.com). DOI 10.1002/cmr.a.20124

THEORY

It is well known that the noise, $N(\boldsymbol{k})$, on the MR signal, $S(\boldsymbol{k})$, can be described as an additive, uncorrelated, complex contribution to the pure MR signal (*1*). Therefore, $S(\boldsymbol{k})$ can be expressed as

$$S(\boldsymbol{k}) = S_{\mathrm{R}}(\boldsymbol{k}) + N_{\mathrm{R}}(\boldsymbol{k}) + j[S_{\mathrm{I}}(\boldsymbol{k}) + N_{\mathrm{I}}(\boldsymbol{k})], \qquad [1]$$

where $j = \sqrt{-1}$, $\boldsymbol{k}$ is the location parameter of the domain in which the signal is acquired, $S_{\mathrm{R}}(\boldsymbol{k})$ and $S_{\mathrm{I}}(\boldsymbol{k})$ are the real and imaginary components of the true (i.e., noiseless) raw signal, respectively, and $N_{\mathrm{R}}(\boldsymbol{k})$ and $N_{\mathrm{I}}(\boldsymbol{k})$ are the real and imaginary noise contributions, respectively. The elements of $N_{\mathrm{R}}(\boldsymbol{k})$ and $N_{\mathrm{I}}(\boldsymbol{k})$ are independent, identically distributed and follow a Gaussian distribution with zero mean and standard deviation, σ_{G} (*2*, *3*). The primary sources of noise in MR are electronic (i.e., Johnson noise) and dielectric and inductive coupling to the conducting solution inside the body (*4*). Importantly, these physical contributions to the noise are independent of the magnitude of the magnetization. The noise can generally be considered to be white noise that is both stationary and ergodic. Other contributions to the noise, such as those derived from the quantization process (*5*), are not considered in this analysis.

The Signal in the Image Domain

The MR signal induced in the receiver coil is a continuous complex signal acquired in a frequency domain commonly referred to as *k*-space. To analyze the MRI data statistics in the image domain, the signal needs to be sampled at discrete locations of *k*-space and then reconstructed using a standard reconstruction algorithm, such as the Inverse Discrete Fourier Transform (IDFT). The reconstructed image, *s*, can be expressed as

$$s = \Im^{-1}\{S\} = \Im^{-1}\{S_{\mathrm{R}} + N_{\mathrm{R}} + j(S_{\mathrm{I}} + N_{\mathrm{I}})\}, \qquad [2]$$

where $\Im^{-1}\{\}$ represents the IDFT. For simplicity, *k*-space is considered to have been sampled at uniform Cartesian locations so that the effects of re-gridding algorithms on the data statistics can be ignored.

Abbreviations

PDF	probability density function
ROI	region of interest
SNR	signal to noise ratio
TE	echo time
IDFT	Inverse Discrete Fourier Transform

Making use of the linearity property of the IDFT, Eq. [2] can be written as

$$s = \Im^{-1}\{S_{\mathrm{R}}\} + j\Im^{-1}\{S_{\mathrm{I}}\} + \Im^{-1}\{N_{\mathrm{R}}\} + j\Im^{-1}\{N_{\mathrm{I}}\} \qquad [3]$$

or

$$s = A_{\mathrm{R}} + jA_{\mathrm{I}} + n_{\mathrm{R}} + jn_{\mathrm{I}}, \qquad [4]$$

where $A_{\mathrm{R}} + jA_{\mathrm{I}} \equiv \Im^{-1}\{S_{\mathrm{R}}\} + j\Im^{-1}\{S_{\mathrm{I}}\}$ corresponds to the reconstructed complex noiseless MR image and $n = n_{\mathrm{R}} + jn_{\mathrm{I}} \equiv \Im^{-1}\{N_{\mathrm{R}}\} + j\Im^{-1}\{N_{\mathrm{I}}\}$ is the complex noise in the image domain. From Eq. [4] it is clear that the noise in the image domain is still additive. Furthermore, the real and imaginary parts of the image noise are still zero mean Gaussian signals (a proof of this is presented in the Appendix) and their PDFs can be written as

$$P(n_{\mathrm{R,I}}) = \frac{1}{\sqrt{2\pi\sigma_{\mathrm{g}}^2}} \exp\left(-\frac{n_{\mathrm{R,I}}^2}{2\sigma_{\mathrm{g}}^2}\right), \qquad [5]$$

where σ_{g} is the standard deviation of the Gaussian noise in the image domain. The corresponding PDFs for s_{R} and s_{I}, the real and imaginary components, respectively, of the reconstructed noisy MR complex image, are given by

$$P(s_{\mathrm{R,I}}) = \frac{1}{\sqrt{2\pi\sigma_{\mathrm{g}}^2}} \exp\left(-\frac{\left(A_{\mathrm{R,I}} - s_{\mathrm{R,I}}\right)^2}{2\sigma_{\mathrm{g}}^2}\right). \qquad [6]$$

Magnitude Images

It is a common practice in MR to work with magnitude images rather than the complex ones. The magnitude image, *m*, is computed as

$$\begin{aligned} m &= \sqrt{(A_{\mathrm{R}} + n_{\mathrm{R}})^2 + (A_{\mathrm{I}} + n_{\mathrm{I}})^2} \\ &= \sqrt{(A\cos\varphi + n_{\mathrm{R}})^2 + (A\sin\varphi + n_{\mathrm{I}})^2}, \end{aligned} \qquad [7]$$

where *A* and φ are the magnitude and phase of the true, noiseless image signal, respectively. Since this is a nonlinear transformation, the distribution of pixel intensities in the resulting image is, in general, not Gaussian; the magnitude operation (*2*, *3*) rectifies low SNR signals causing the noise statistics to change.

Since s_{R} and s_{I} are independent their joint complex PDF can be expressed as the product of their individual PDFs:

$$P(s_R, s_I|A,\varphi,\sigma_g) = \frac{1}{2\pi\sigma_g^2}\exp\left[\frac{-(A\cos\varphi - s_R)^2}{2\sigma_g^2}\right] \times \exp\left[\frac{-(A\sin\varphi - s_I)^2}{2\sigma_g^2}\right]. \quad [8]$$

Changing to polar coordinates gives

$$P(m,\theta|A,\varphi,\sigma_g) = \frac{1}{2\pi\sigma_g^2}\exp\left[\frac{-(A\cos\varphi - m\cos\theta)^2}{2\sigma_g^2}\right] \times \exp\left[\frac{-(A\sin\varphi - m\sin\theta)^2}{2\sigma_g^2}\right] J(m,\theta), \quad [9]$$

where θ is the phase of the reconstructed noisy image signal and the determinant of the Jacobian matrix, *J(m, θ)*, can be computed as:

$$J(m,\theta) = \begin{vmatrix} \frac{\partial s_R}{\partial m} & \frac{\partial s_R}{\partial \theta} \\ \frac{\partial s_I}{\partial m} & \frac{\partial s_I}{\partial \theta} \end{vmatrix} = \begin{vmatrix} \cos\theta & -m\sin\theta \\ \sin\theta & m\cos\theta \end{vmatrix} = m\cos^2\theta + m\sin^2\theta = m. \quad [10]$$

Integrating over a full θ cycle and expanding the polynomials gives the marginal PDF:

$$P_m(m|A,\varphi,\sigma_g) = \frac{m}{2\pi\sigma_g^2}\int_0^{2\pi}\exp\left[\frac{-A^2(\sin^2\varphi + \cos^2\varphi)}{2\sigma_g^2}\right] \times \exp\left[\frac{-m^2(\sin^2\theta + \cos^2\theta)}{2\sigma_g^2}\right] \times \exp\left[\frac{-2Am(\cos\varphi\cos\theta + \sin\varphi\sin\theta)}{2\sigma_g^2}\right]d\theta \quad [11]$$

or

$$P_m(m|A,\varphi,\sigma_g) = \frac{m}{2\pi\sigma_g^2} \times \int_0^{2\pi}\exp\left[\frac{-(A^2 + m^2 - 2Am\cos(\theta - \varphi))}{2\sigma_g^2}\right]d\theta, \quad [12]$$

where the subscripted "*m*" indicates that the PDF is for the magnitude of the signal only. Since the phase, φ, is a constant unaffected by the noise and the integration in Eq. [12] is over a full cycle of a cosine function, φ can be dismissed, giving:

$$P_m(m|A,\sigma_g) = \frac{m}{2\pi\sigma_g^2}\exp\left[-\frac{(A^2 + m^2)}{2\sigma_g^2}\right] \times \int_0^{2\pi}\exp\left[\frac{Am\cos\theta}{\sigma_g^2}\right]d\theta. \quad [13]$$

This can also be written in terms of the 0th order modified Bessel function of the first kind since:

$$I_0(z) = \frac{1}{2\pi}\int_0^{2\pi}\exp[z\cos(\alpha)]d\alpha. \quad [14]$$

Therefore, the PDF for a noisy magnitude MR image (as shown by Bernstein et al. (*6*)) is given by:

$$P_m(m|A,\sigma_g) = \frac{m}{\sigma_g^2}\exp\left[-\frac{(A^2 + m^2)}{2\sigma_g^2}\right]I_0\left(\frac{Am}{\sigma_g^2}\right)H(m), \quad [15]$$

where *H(m)* is the Heaviside step function, which is included in this expression to ensure mathematically that the PDF is zero for negative values of *m*.

Equation *15* describes the Rician PDF (*7*) that characterizes the distribution of MR pixel intensities for most standard situations. Importantly, this function does not, in general, describe the distribution of noise in the image—it is the distribution of pixel intensities observed in the presence of noise. A few MR imaging techniques such as "phase contrast" and "parallel imaging" result in slightly different PDFs (*8*, *9*).

Properties of the Rician Distribution

The Rician PDF has different characteristics, depending on the true noiseless signal strength, *A*. As stated by Edelstein et al. (*10*) and later on by Gudbjartsson and Patz (*3*), among others, in the absence of an MR signal (i.e., when $A = 0$), the Rician PDF reduces to a Rayleigh PDF:

$$P_m(m|\sigma_g) = \frac{m}{\sigma_g^2}\exp\left[-\frac{m^2}{2\sigma_g^2}\right]H(m). \quad [16]$$

The mean, $\langle m \rangle_{\mathrm{Ray}}$, and standard deviation, σ_{Ray}, for the Rayleigh PDF are given by:

$$\langle m \rangle_{\mathrm{Ray}} = \sigma_{\mathrm{g}} \sqrt{\frac{\pi}{2}} \qquad [17]$$

and

$$\sigma_{\mathrm{Ray}} = \sigma_{\mathrm{g}} \sqrt{2 - \frac{\pi}{2}}, \qquad [18]$$

respectively. For high values of A/σ_{g} the Rician PDF behaves like a Gaussian PDF:

$$P_{\mathrm{m}}(m|\mathrm{A},\sigma_{\mathrm{g}}) \approx \frac{1}{\sigma_{\mathrm{g}}\sqrt{2\pi}} \exp\left[-\frac{\left(m-\sqrt{A^2+\sigma_{\mathrm{g}}^2}\right)^2}{2\sigma_{\mathrm{g}}^2}\right] H(m). \qquad [19]$$

This behavior can be seen in Fig. 1, where Rician PDFs are shown for different values of A/σ_{g}. When A/σ_{g} is small, the mean of the Rician PDF, $\langle m \rangle_{\mathrm{Rice}}$, differs significantly from the true signal magnitude, A. As A/σ_{g} increases, the Rician PDF starts to resemble a Gaussian PDF, and $\langle m \rangle_{\mathrm{Rice}}$ becomes a better approximation of A. It should also be noted that the width of the Rician distribution is a function of both A and σ_{g}.

The inequality of $\langle m \rangle_{\mathrm{Rice}}$ and the magnitude of the true signal A, has been described by several authors (*2*, *3*, *11*, *12*) since it produces a bias in low SNR MR magnitude values which can lead to inaccuracies in the quantitative determination of MR parameters such as the spin-spin relaxation time, T_2, and the apparent diffusion coefficient among others (*8*, *13*, *14*). This bias is sometimes referred to as the "*Rician noise bias*". Several methods for compensating for this effect have been proposed (*2*, *3*, *11*, *12*, *13*); however, discussion of these topics is beyond the scope of this article.

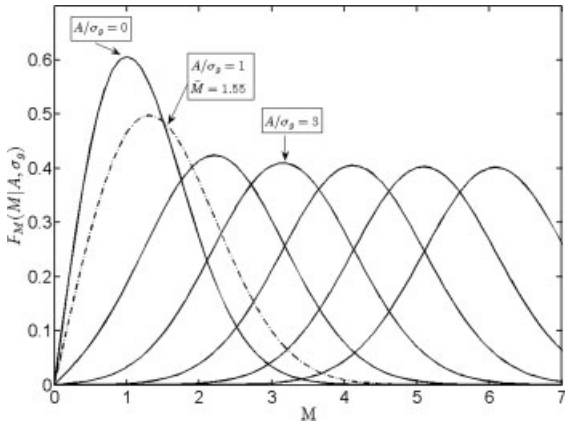

Figure 1 The Rician probability density function (Eq. [3]) plotted for several values of A/σ_{g}. These PDFs show the transition from the Rayleigh PDF obtained for $A = 0$ to a Gaussian shaped PDF as the value of A increases. The second curve ($A/\sigma_{\mathrm{g}} = 1$), plotted as a dashed line, illustrates how, for low A/σ_{g} values, the magnitude of the true signal ($A = 1$) differs quite significantly from the mean of the Rician PDF ($M = 1.55$).

DISCUSSION

The use of the term *Rician noise* suggests that the magnitude of the noise be equated with σ_{r}, the standard deviation of the Rician PDF. Noise defined in this way is a function of A even though, as noted above, the actual physical contributions to the noise do not depend on A. The A-dependence of σ_{r} (*12*) is introduced by the signal rectification that occurs when the magnitude calculation is performed; it does not have a physical source. This terminology is misleading and can cause confusion.

One consequence of this concept of *Rician noise* is that images corresponding to different TEs, for example, but for which the acquisition procedure was otherwise identical, would have different *Rician noise* contributions, even though the physical contributions to the noise have not changed. Another consequence is that, in general, the noise characteristics will change from pixel to pixel in the same image. For example, in a standard head image the *Rician noise* characteristics (i) in the background, (ii) in the brain parenchyma, and (iii) in the cerebrospinal fluid will all be different, even though it is the same image.

A further complication with this concept of *Rician noise* is that σ_{r} does not relate uniquely to the physical sources of noise since σ_{r} depends on both A and σ_{g}. In other words, a measured value of σ_{r} does not correspond to a specific value of σ_{g} since there are many combinations of A and σ_{g} that produce the same σ_{r} value. The width of the pixel intensity distribution for a given value of A is characterized by σ_{r}, but to consider this to be noise when a unique relationship with the physical sources of the noise does not exist, is inadvisable.

A better approach when dealing with noise in MR magnitude images is to relate it back to the Gaussian noise on the real and imaginary signals. The standard deviation of the Gaussian noise can readily be determined by implementing the automatic algorithm

recently described in the literature by Sijbers et al. (*15*) for calculating the mean or standard deviation for a region of interest (ROI) located in the background of a magnitude image where $A = 0$; as described by Andersen (*16*). In this special case, the Rician PDF reduces to a Rayleigh PDF and σ_g can easily be determined from either the mean or the standard deviation of the ROI (using Eqs. [17] or [18]), assuming that the ROI has been carefully chosen to avoid artefacts. In our experience it is better to use the mean value since it is less likely to be affected by processes such as Hanning filtering that may be part of the image reconstruction process. Noise determined in this way (e.g., from a background ROI) is independent of A and it has a unique relationship with the physical sources of the noise. It is a more meaningful quantity and its physical properties are more consistent with the behaviour normally associated with noise.

Another common misconception is that the noise in MR magnitude images is "Rayleigh Noise" (e.g., see (*17–19*)). It is true that when $A = 0$ the Rician distribution reduces to a Rayleigh distribution and, since there is no MR signal, this corresponds to the noise distribution in this case. However, noise also exists when $A > 0$ and the noise induced uncertainties in the measured signals for this case do not correspond to a Rayleigh distribution.

With the conventional concept of noise, the measured value of a quantity corresponds to the true value, A, plus a contribution due to noise (see Eq. [3]). Thus, for Gaussian noise the distribution of measured values will also be Gaussian with the same standard deviation for all values of A. For a Rician PDF, this simple additive relationship between A and the noise induced width of the PDF does not exist since the shape of the distribution changes considerably with the value of A (see Fig. 1).

The mean of the Rician PDF is not, in general, equal to A. This difference is sometimes referred to as "*Rician noise bias*" or, when $A = 0$, as the "*Rician noise floor*". However, this bias is a consequence of the asymmetry of the Rician (or Raleigh) PDF when the SNR is low and is not directly related to σ_r. Consequently, "*Rician bias*", "*Rician* (*or Rayleigh*) floor" and "rectified noise bias" would be more appropriate terminology for this effect.

The discussion presented here has been limited to the case where the signal was acquired with a conventional quadrature receive coil. For the more general situation, where a phased array coil is used for signal detection, the PDF in the image domain is a non-central Chi distribution (*9*) rather than a Rician distribution. However, when the number of coils in the phased array is small and when the SNR is low, the PDF is asymmetric and is similar to the Rician PDF. As a result, many of the comments made in the discussion above for quadrature signal detection also apply when phased array coils are used.

CONCLUSIONS

Noise on real and imaginary MR signals is Gaussian but it manifests itself in magnitude images as a Rician distribution of pixel intensities. For Gaussian noise it is common practice to consider the "magnitude" of the noise to be the standard deviation of the Gaussian PDF. Correspondingly, the use of the expression "*Rician noise*" suggests that the magnitude of the noise should be set equal to σ_r, the standard deviation of the Rician PDF. However, noise defined in this way has unusual properties such as the noise magnitude being a function of A, the true noiseless pixel intensity, and not having a unique relationship to the physical sources of the noise. Therefore, it is our contention that the use of the term "*Rician noise*" causes confusion and should be avoided. A better approach when dealing with noise in MR magnitude images is to relate it back to σ_g, the Gaussian noise on the real and imaginary image signals. Furthermore, the difference between the mean of the Rician PDF and A should be referred to as "*Rician bias*" rather than "*Rician noise bias*" since it is due to the asymmetry of the Rician PDF and not its width.

NOMENCLATURE

A	Magnitude of the true MR signal
A_I	Real component of true MR signal
A_R	Imaginary component of the true MR signal
$\Im^{-1}$	Inverse descrete Fourier transform
H(m)	Heaviside function
I_0	Modified zeroth order Bessel function of the first kind
J	Jacobian matrix
j	Imaginary unit
k	Location parameter of the domain in which the MR signal is acquired (k-space)
m	Magnitude value of the image
$\langle m \rangle$	Mean of measured magnitude value
N_R	Real component of the noise in k-space
N_I	Imaginary component of the noise in k-space
n	Noise in the image domain

n_R Real component of the noise in the image domain
n_I Imaginary component of the noise in the image domain
p() Probability density function
S Signal of a pixel in k-space
S_R Real component of the signal of a pixel in k-space
S_I Imaginary component of the signal of a pixel in k-space
s Signal of a pixel in the image domain
φ Phase of the true MR image
σ_G Standard deviation of the background Gaussian noise in k-space
σ_g Standard deviation of the background Gaussian noise in the image domain
θ Phase of the noisy MR image

APPENDIX

The purpose of this appendix is to show that, when the real and imaginary parts of the noise in k-space, N_R and N_I, respectively, are both zero mean Gaussian random variables, the PDFs of their IDFTs are also zero mean Gaussian PDFs.

The IDFT of the complex Gaussian noise in k-space can be written:

$$n(x) = \Im^{-1}\{N_R + jN_I\} = \frac{1}{L}\sum_{k=0}^{L-1}(N_R(k) + jN_I(k))\exp\left[\frac{j2\pi xk}{L}\right], \quad [A.1]$$

where L is the number of k-space samples. For simplicity, a 1D IDFT is used here since the extension to 2D and 3D is straight forward. The PDFs for N_R and N_I are given by:

$$P(N_R) = G_{N_R}\left(0, \sigma_G^2\right) \equiv \frac{1}{\sqrt{2\pi\sigma_G^2}}\exp\left[-\frac{N_R^2}{2\sigma_G^2}\right] \quad [A.2]$$

and

$$P(N_I) = G_{N_I}\left(0, \sigma_G^2\right) \equiv \frac{1}{\sqrt{2\pi\sigma_G^2}}\exp\left[-\frac{N_I^2}{2\sigma_G^2}\right], \quad [A.3]$$

respectively, where the shorthand notation $G_x(\mu,\sigma^2)$ has been introduced to designate a Gaussian PDF with a mean of μ and with a variance of σ^2, for the variable x. It should be noted that since $P(N_R)$ and $P(N_I)$ are Gaussian PDFs with the same mean and variance, these functions are clearly equal, even though they have been expressed above in terms of different "dummy" variables. The probability of getting a specific value for N_R in a single measurement is identical to the probability of getting the same value for N_I in a single measurement. In the following the subscript will be dropped unless its inclusion adds clarity.

Equation [A.1] can be written in terms of its real and imaginary parts using Euler's formula for complex numbers, $e^{j\theta} = \cos\theta + j\sin\theta$. The result can be expressed as:

$$n(x) = n_R(x) + jn_I(x) = \frac{1}{L}\sum_{k=0}^{L-1}(p(k) + jq(k)), \quad [A.4]$$

where

$$p(k) \equiv (N_R(k)\cos\theta_k - N_I(k)\sin\theta_k), \quad [A.5]$$

$$q(k) \equiv (N_I(k)\cos\theta_k + N_R(k)\sin\theta_k) \quad [A.6]$$

and

$$\theta_k \equiv \frac{2\pi xk}{L}. \quad [A.7]$$

To determine the PDF for $p(k)$ the following properties of Gaussian PDFs can be used (*20*):

i. If x is a Gaussian random variate corresponding to the PDF $G_x(\mu,\sigma^2)$, then cx is also a Gaussian random variate and its PDF is $G_{cx}(c\mu,c^2\sigma^2)$, where c is a real constant.
ii. If x_i are independent Gaussian random variates corresponding to the PDFs $G_{x_i}(\mu_{x_i}, \sigma_{x_i}^2)$ then $y = \sum_i x_i$ is also a Gaussian random variate and its PDF is $G_y\left(\sum_i \mu_{x_i}, \sum_i \sigma_{x_i}^2\right)$.

For a specific location, x, in image space, θ_k evaluates to a real constant which, in general, is different for each term in the expansion. Thus, by property i), the two terms in $p(k)$ are each Gaussian variates with PDFs given by $G_{N_R\cos\theta_k}\left(0, \sigma_G^2\cos^2\theta_k\right)$ and $G_{N_I\sin\theta_k}\left(0, \sigma_G^2\sin^2\theta_k\right)$, respectively. From property ii) it can now be seen that $p(k)$ is a Gaussian variate and its PDF is:

$$P(p(k)) = G_{p(k)}\left(0, \sigma_G^2\cos^2\theta_k + \sigma_G^2\sin^2\theta_k\right) = G\left(0, \sigma_G^2\right). \quad [A.8]$$

Similarly, it can be shown that $q(k)$ is a Gaussian random variate and its PDF is

$$P(q(k)) = G\left(0, \sigma_G^2\right). \quad [A.9]$$

By applying property ii) to deal with the sum and then property i) to deal with the constant factor it can also be seen that $n_R(x)$ and $n_I(k)$ are Gaussian random variates and their PDFs are given by:

$$P(n_R(x)) = P\left(\frac{1}{L}\sum_{k=0}^{L-1} p(k)\right) = G\left(0, \frac{\sigma_G^2}{L}\right) \quad [A.10]$$

and

$$P(n_I(x)) = P\left(\frac{1}{L}\sum_{k=0}^{L-1} q(k)\right) = G\left(0, \frac{\sigma_G^2}{L}\right), \quad [A.11]$$

respectively. This is the desired result.

ACKNOWLEDGMENTS

A.C-B. and I.C. thank the Ontario Research and Development Challenge Fund for financial support, the Ottawa Health Research Institute, and Dr. Greg O. Cron. C.T. thanks his grant sponsor Fondecyt (#1060008) for their support.

REFERENCES

1. Wang Y, Lei T. 1994. Statistical analysis of MR imaging and its applications in image modelling. Proceedings of the IEEE International conference on Image Processing and Neural Networks 1:866–870.
2. Henkelman RM. 1986. Measurement of signal intensities in the presence of noise in MR images. Med Phys 12:232–233. Erratum in 1986;13:544.
3. Gudbjartsson H, Patz S. 1995. The Rician distribution of noisy MRI data. Magn Reson Med 34:910–914. Erratum in Magn Reson Med 1996;36(2):332–333.
4. Chen CN, Hoult DI. 1989. Signal and noise. In: Biomedical Magnetic Resonance Technology. Bristol and New York: Adam Hilger. pp 117–176.
5. Cádiz RF, Tejos CA, Irarrazaval P, Guarini M. 2007. Quantization noise in MRI acquisition. In: Proceedings of the 15th Annual Meeting of ISMRM-ESMRMB, Berlin. p 658.
6. Bernstein MA, Thomasson DM, Perman WH. 1989. Improved detectability in low signal-to-noise ratio magnetic resonance images by means of a phase–corrected real reconstruction. Med Phys 16:813–817.
7. Rice SO. 1944. Mathematical analysis of random noise. Bell Syst Technol J 23:282–332.
8. Andersen AH, Kirsch JE. 1996. Analysis of noise in phase contrast MR imaging. Med Phys 23:857–869.
9. Constantinides CD, Atalar E, McVeigh ER. 1997. Signal-to-noise measurements in magnitude images from NMR phased arrays. Magn Reson Med 38:852–857.
10. Edelstein WA, Bottomley PA, Pfeifer LM. 1984. A signal-to-noise calibration procedure for NMR imaging systems. Med Phys 11:180–185.
11. Miller AJ, Joseph PM. 1993. The use of power images to perform quantitative analysis on low SNR MR images. Magn Reson Imag 11:1051–1056.
12. Koay CG, Basser PJ. 2006. Analytically exact correction scheme for signal extraction from noisy magnitude MR signals. J Magn Reson 179:317–322.
13. Cárdenas-Blanco A, Nezamzadeh M, Foottit C, Cameron I. 2007. Accurate noise bias correction applied to individual pixels. In: Proceedings of the 15th Annual Meeting of ISMRM-ESMRMB, Berlin. p 657.
14. Jones DK, Basser PJ. 2004. "Squashing peanuts and smashing pumpkins": How noise distorts diffusion weighted MR data. Magn Reson Med 52:979–993.
15. Sijbers J, Poot D, Dekker AJ, Pintjens W. 2007. Automatic estimation of the noise variance from the histogram of a magnetic resonance image. Phys Med Biol 52:1335–1348.
16. Andersen AH. 1996. On the rician distribution of noisy MRI data. Magn Reson Med 36:331–333.
17. Feinberg DA, Rofsky NM, Johnson G. 1995. Multiple Breat-hold averaging (MBA) method for increasing SNR in abdominal MRI. Magn Reson Med 34:905–909.
18. Wheeler-Kingshott CAM, Parker GJM, Symms MR, Hickman SJ, Tofts PS, Miller DH, et al. 2002. ADC mapping of the human optic nerve: Increased resolution, coverage, and reliability with CSF-suppressed ZOOM-EPI. Magn Reson Med 47:24–31.
19. Hickman SJ, Wheeler-Kingshott CAM, Jones SJ, Miszkiel KA, Barker GJ, Plant GT, et al. 2005. Optic nerve diffusion measurement from diffusion-weighted imaging in optic neuritis. Am J Neuroradiol 26:951–956.
20. Normal Sum Distributions, http://mathworld.wolfram.com/NormalSumDistribution.html. June 4, 2008.

BIOGRAPHIES

Arturo Cárdenas-Blanco was born in the last century in Seville, Spain. He received his M.Sc. in medical physics from the University of Hull, Kingston upon Hull, UK. Following that, he moved to Cambridge, where he did his Ph.D. with Professor Laurance D. Hall at the Herchel Smith Laboratory for Medicinal Chemistry. He spent two years working with Dr. Ian Cameron as a post-doc at the Ottawa Health Research Institute (OHRI), and now he is a postdoctoral fellow with Dr. Eve Tsai in the Division of Neuroscience at the OHRI. His research interests include spinal cord imaging, brain imaging, cartilage imaging, noise reduction, diffusion imaging, and fiber tractography.

Cristian Tejos received his B.Sc. and M.Sc. in electrical engineering in 2000 from the Pontificia Universidad Catolica de Chile. Shortly after, he moved to the United Kingdom to complete his academic training. Firstly, he received M.Sc. in engineering and physical science in medicine from the Department of Bioengineering at Imperial College London, UK. Secondly, he received a Ph.D. from the School of Clinical Medicine at the University of Cambridge, UK. In 2005, he returned to Chile to work as a postdoctoral fellow at the Biomedical Imaging Center, Pontificia Universidad Catolica de Chile, where he is now a research associate. In 2005, he became assistant professor of the Department of Electrical Engineering of the same university. His main research interests are in image processing, with specific emphasis in the development of image segmentation techniques, and in magnetic resonance imaging, especially in the design of reconstruction algorithms for under-sampled data.

Pablo Irarrazaval received his B.Sc. in electrical engineering in 1988 from the Pontificia Universidad Catolica de Chile (PUC), and his M.Sc. and Ph.D. from Stanford University. He is a Professor with the Electrical Engineering Department at PUC and director of the Biomedical Imaging Center. He was chairman of the Department and Vice-Dean of Academic Affairs of the College of Engineering at PUC. His research interest is in Medical Imaging, particularly with Magnetic Resonance Imaging acquisition and reconstruction, and with Image Perception.

Ian Cameron obtained his B.Sc. in physics and mathematics from the University of Prince Edward Island followed by his M.Sc. and Ph.D. in Physics from the University of Waterloo under the supervision of Prof. Mik Pintar. Following graduation he worked as a Visiting Fellow in a Canadian Government Laboratory in the Chemistry Division of the National Research Council of Canada. He is currently the MR Physicist at The Ottawa Hospital, an Assistant Professor in the Radiology Department at the University of Ottawa as well as an Adjunct Research Professor in the Physics Department at Carleton University and he is a Fellow of the Canadian College of Physicists in Medicine.